



<b>Publication Year</b>	2016
<b>Acceptance in OA</b>	2020-05-05T08:49:52Z
<b>Title</b>	Design, development, and performance of the fibres of MOONS
<b>Authors</b>	Guinouard, Isabelle, Avila, Gerardo, Lee, David, Amans, Jean-Philippe, Rees, Phil, Taylor, William, OLIVA, Ernesto
<b>Publisher's version (DOI)</b>	10.1117/12.2231413
<b>Handle</b>	<a href="http://hdl.handle.net/20.500.12386/24474">http://hdl.handle.net/20.500.12386/24474</a>
<b>Serie</b>	PROCEEDINGS OF SPIE
<b>Volume</b>	9912

# PROCEEDINGS OF SPIE

[SPIDigitalLibrary.org/conference-proceedings-of-spie](https://spiedigitallibrary.org/conference-proceedings-of-spie)

## Design, development, and performance of the fibres of MOONS

Guinouard, Isabelle, Avila, Gerardo, Lee, David, Amans, Jean-Philippe, Rees, Phil, et al.

Isabelle Guinouard, Gerardo Avila, David Lee, Jean-Philippe Amans, Phil Rees, William Taylor, Ernesto Oliva, "Design, development, and performance of the fibres of MOONS," Proc. SPIE 9912, Advances in Optical and Mechanical Technologies for Telescopes and Instrumentation II, 99125G (22 July 2016); doi: 10.1117/12.2231413

**SPIE.**

Event: SPIE Astronomical Telescopes + Instrumentation, 2016, Edinburgh, United Kingdom

# Design, development and performance of the fibres of MOONS

Isabelle Guinouard<sup>\*a</sup>, Gerardo Avila<sup>b</sup>, David Lee<sup>c</sup>, Jean-Philippe Amans<sup>a</sup>,  
Phil Rees<sup>c</sup>, William Taylor<sup>c</sup>, Ernesto Oliva<sup>d</sup>

<sup>a</sup> GEPI, Observatoire de Paris-CNRS-Université Paris Diderot-Paris Sciences et Lettres,  
5 Pl. Janssen, 92195 Meudon, France;

<sup>b</sup> ESO, Karl-Schwarzschild-Str. 2 85748 Garching bei München, D;

<sup>c</sup> UKATC, Royal Observatory, Blackford Hill, Edinburgh, EH9 3HJ, UK;

<sup>d</sup> INAF, Osservatorio Astrofisico di Arcetri 50125 Firenze, IT;

## ABSTRACT

The Multi-Object Optical and Near-infrared Spectrograph (MOONS) will exploit the full 500 square arcmin field of view offered by the Nasmyth focus of the Very Large Telescope and will be equipped with two identical triple arm cryogenic spectrographs covering the wavelength range 0.64 $\mu$ m-1.8 $\mu$ m, with a multiplex capability of over 1000 fibres. Each spectrograph will produce spectra for 500 targets simultaneously, each with its own dedicated sky fibre for optimal sky subtraction. The system will have both a medium resolution (R~4000-6000) mode and a high resolution (R~20000) mode.

The fibres are used to pick off each sub field of 1" and are used to transport the light from the instrument focal plane to the two spectrographs. Each fibre has a microlens to focus the beam into the fibre at a relative fast focal ratio of F/3.65 to reduce the Focal Ratio Degradation (FRD).

This paper presents the design of the fibre management module and describes the specific developments required to optimise its performances.

**Keywords:** MOONS, VLT, Optical fibres, Multi Object Spectroscopy

## 1 INTRODUCTION

MOONS is described in several papers of which "MOONS: an optical and near-IR multi-object spectrograph for the Very Large Telescope" (Cirasuolo et al.) [1] is the most important. Fibres are used to pick off each sub field and are used to transport the light from the instrument focal plane to the two spectrographs. The distance between the two determined the length of the fibre assemblies which in the current design is in the order of 10m. A schematic view of this system is shown in Figure 1.

---

\* Contact: Isabelle.Guinouard@obspm.fr; phone +33-1-45077983; fax +33-1-45077709. GEPI, Observatoire de Paris

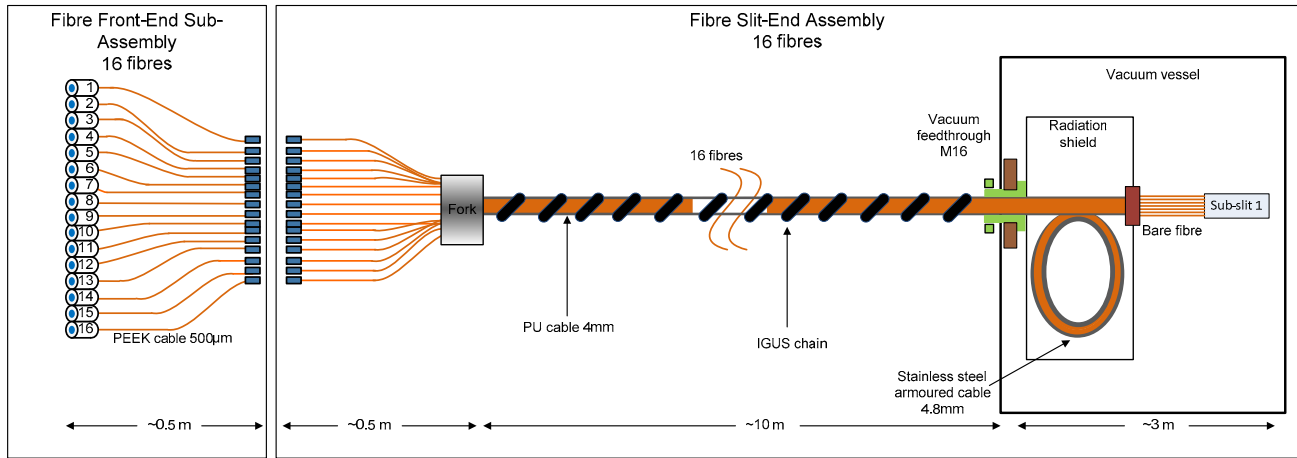


Figure 1 Bundle design

## 2 PRELIMINARY DESIGN

### 2.1 Fibre button optical design description

To comply with the science requirements, each fibre shall have an on-sky aperture  $\geq 1$  arcsec. The aperture is adapted by a single microlens glued onto a fibre with a core diameter of  $150\ \mu\text{m}$ . This lens will also help to limit the loss of light and is also required to speed up to focal ratio such that the output of the fibres will match the spectrograph's input focal ratio of F/3.5. The optical aperture conversion at the input of each fibre is shown in Figure 2. Thus in MOONS, we inject at a fast F ratio of F/3.65, which limits the FRD. At the output, the F ratio is slightly degraded and is at F/3.5.

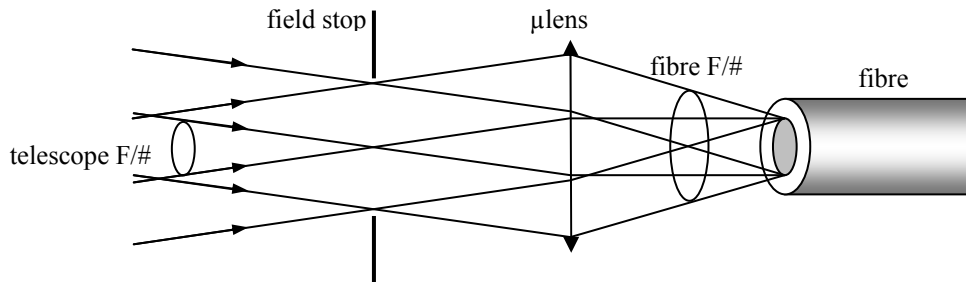


Figure 2 Fibre injection principle (pupil image on fibre core)

The field is defined by the field stop located in the object focal plane of the microlens. The microlens projects the image of the pupil (primary mirror) onto the fibre core. The projected beams from all points in the image plane are injected into the fibre with the same F/number because the field is located in the object focal plane of the microlens. The diameter of the size of the pupil is  $142\ \mu\text{m}$  (diameter fibre core:  $150\ \mu\text{m}$ ).

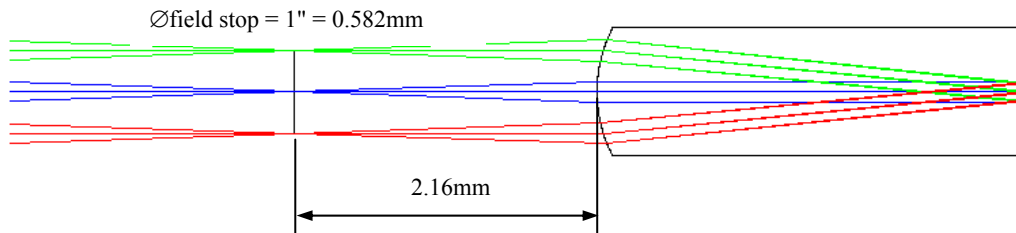


Figure 3 Microlens design

Glass = fused silica ( $n_d = 1.458464$ )  
 Radius of curvature = 0.975mm (Zemax optimization)  
 Thickness = 3.08mm  
 Diameter = 0.9mm  
 AR coating on the spherical surface  
 Spectral bandwidth = 0.6 - 1.8 $\mu$ m

## 2.2 Fibre selection

Only Polymicro were investigated, Polymicro fibres are well known and are used in various astronomical instruments. The wavelength coverage for MOONS is from 0.64  $\mu$ m to 1.8  $\mu$ m, the FIP fibre is chosen, with the expected attenuation as shown in Fig. 4.

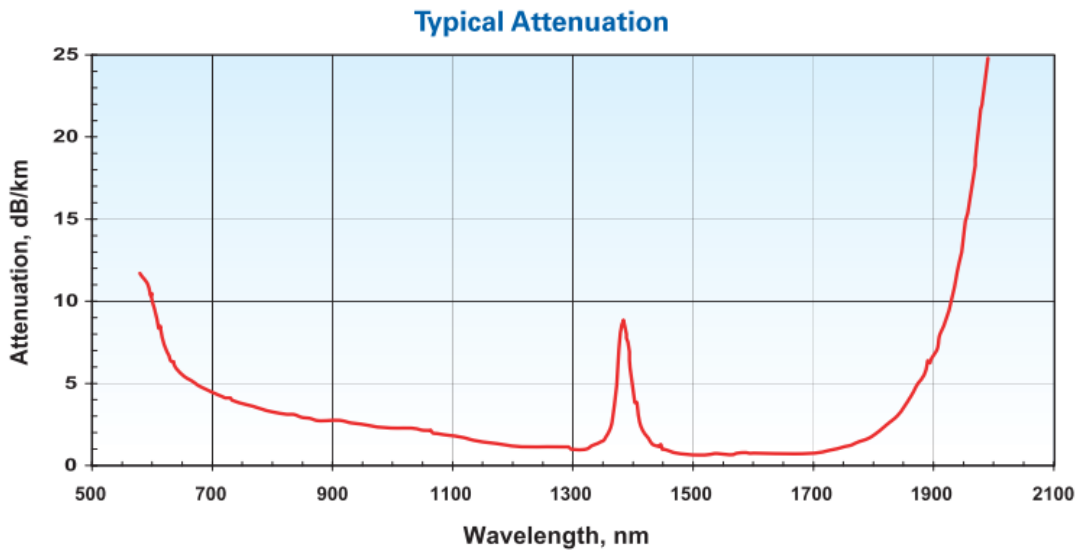


Figure 4 Data sheet from Polymicro(Molex)

In order to optimize the performance of the fibre and so to decrease the Focal Ratio Degradation (FRD), the ratio between the core and the cladding is 1.2, resulting in a fibre design as shown in Fig. 5. This ratio is also chosen to avoid evanescent wave losses in the cladding.

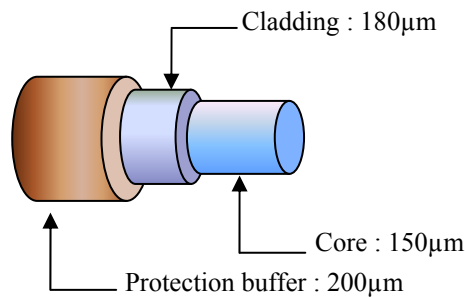


Figure 5 Structure of the fibre

The FRD is the decrease in focal ratio (decrease in effective F-number) in an optical fibre. The ability of a fibre to preserve the angular distribution of the input beam from the telescope to the spectrograph is very important in order to maintain a feasible spectrograph size with good efficiency.

The major causes of FRD are mechanical variations in the fibre dimensions with length (under the manufacturer's control) and the mechanical set-up of the instrumentation (under the control of the user). Small variations in the fibre core diameter or core-clad interface can cause mode stripping, resulting in FRD. Both macro bending and micro bending will cause FRD.

### 2.3 Front-end assembly

The fibre button needs to be attached to the fibre positioning arm, as shown in Fig. 6. The curved arm holds the cylindrical (button) which is 2.8 mm in diameter and 10.0 mm long. The field stop is located in the object focal plane of the microlens. A small countersink screw clamps the cylindrical button in place.

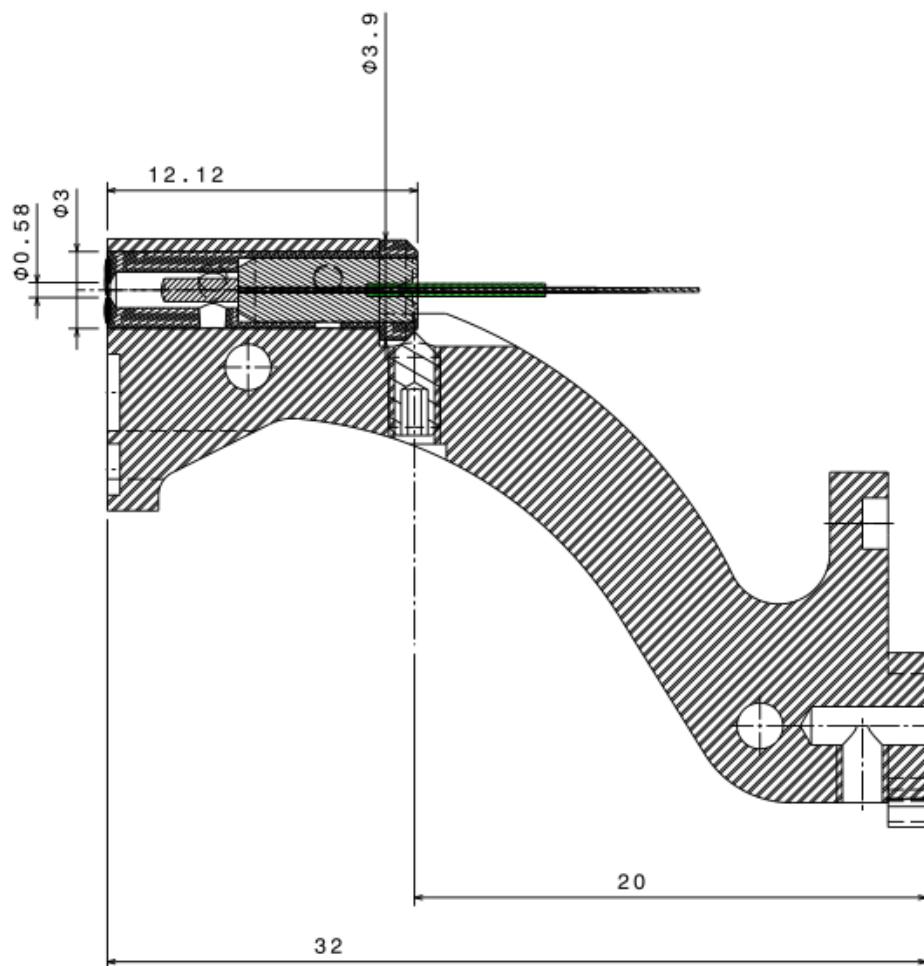


Figure 6 Preliminary design of the fibre button and positioning arm

### 2.4 Slit-end assembly

For the cross-talk considerations, the fibres need a large relative spacing (spacing/size of the fibre core). The minimum spacing between 2 fibres is 5 dark pixels, i.e.  $2.66 \times \phi$  fibre core diameter, as shown below.

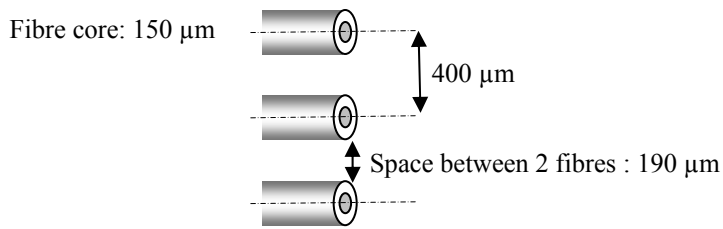


Figure 7 Distance between fibres at the slit

These extremities have to guarantee a good parallelism and a good alignment of the fibres to optimise the coupling with the spectrograph. The fibres are cemented in the mechanical sub-slit and polished (flat polishing). Each sub-slit consists of 16 fibres (see Figure 8).

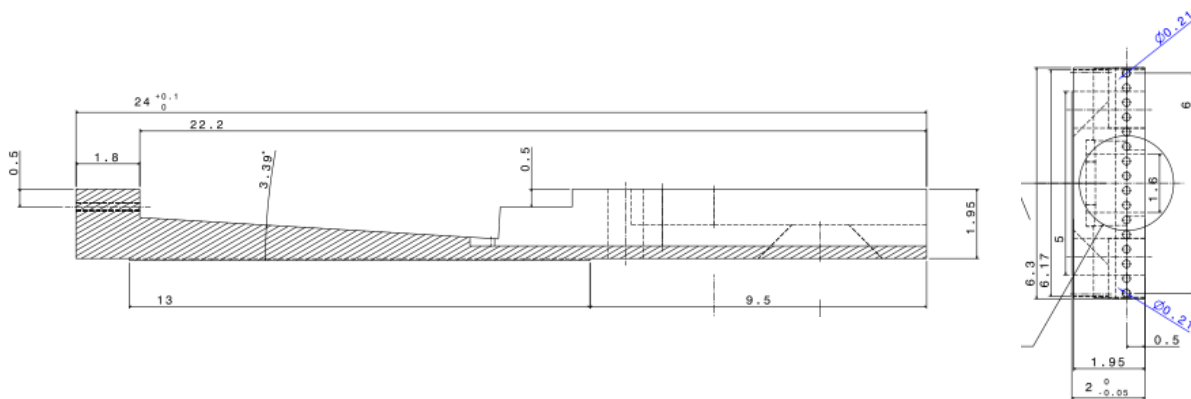


Figure 8 Preliminary design of the sub-slit

### 3 DEVELOPMENT

A full end-to-end prototype, with each component of the design in order to check the feasibility, and better understand the performance of the fibre link, has been manufactured. The design of the prototype fibre system is presented below (Fig. 9) and the manufactured hardware is shown in Fig. 10.

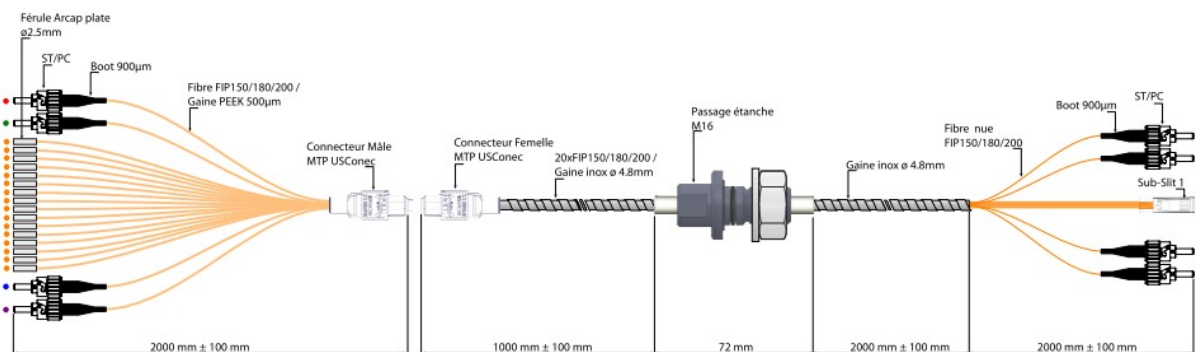


Figure 9 Scheme of the fibre prototype

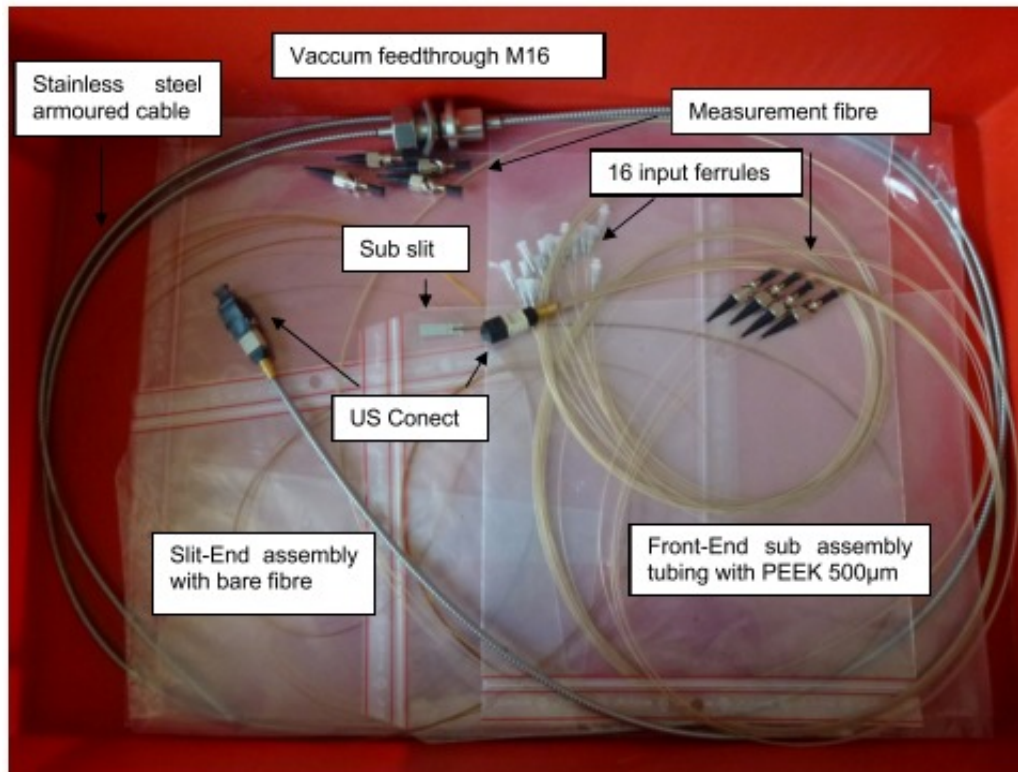


Figure 10 Picture of the fibre prototype

No difficulties were encountered by SEDI on the manufacturing on this bundle of 16 fibres.

The position of the connector along the fibre link is still under discussion. In order to facilitate the integration of one thousand fibres at the front end level, a single connector, shown in Fig. 11, will be placed behind the focal plate.

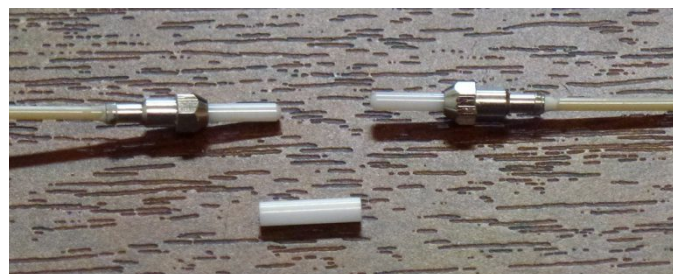


Figure 11 Ferrule mating sleeve

In future other tests will be performed with the ferrule mating sleeve to further investigate the performance.

## 4 PERFORMANCE

### 4.1 FRD measurement

The test bench used for the FRD measurement is described below in Fig. 12, ref [4]. The shape of the projected spot is flat and its size is  $\text{Ø}100\mu\text{m}$  for a fibre core of  $\text{Ø}150\mu\text{m}$ . The centering of the spot on the fibre core is checked using a

viewing system. The transmission is measured in two sequences, first with a direct measurement of the spot, and second the measurement after the slit.

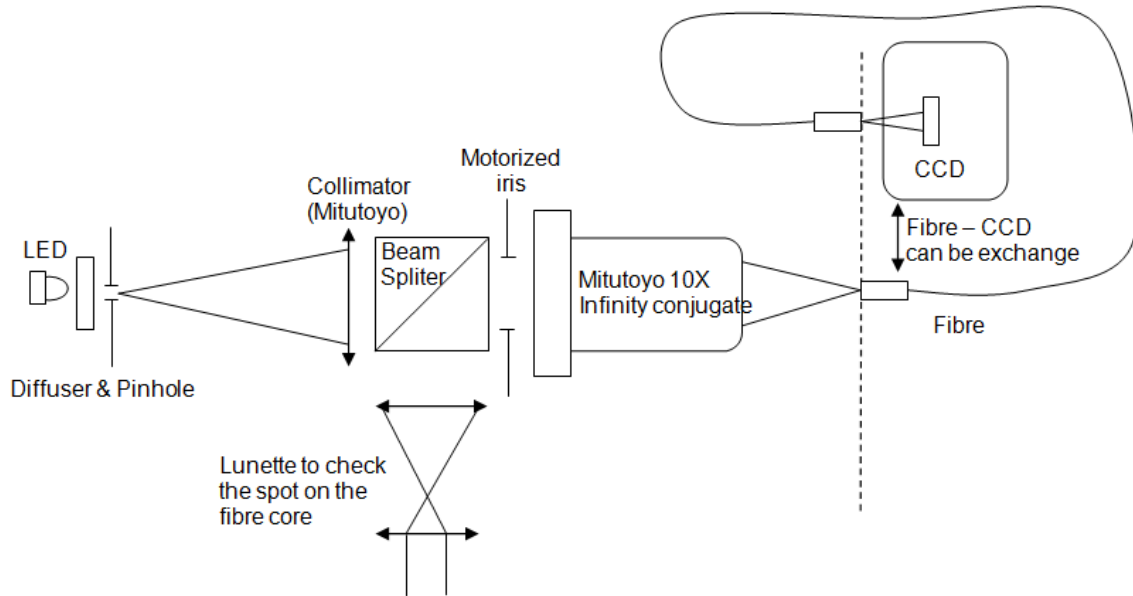


Figure 12 FRD measurement bench

The tested fibre is Polymicro FIP 150/180/200 $\mu\text{m}$ . A first measurement has been done on a sample of bare fibre at 530nm and the FRD results are shown in Fig. 13.

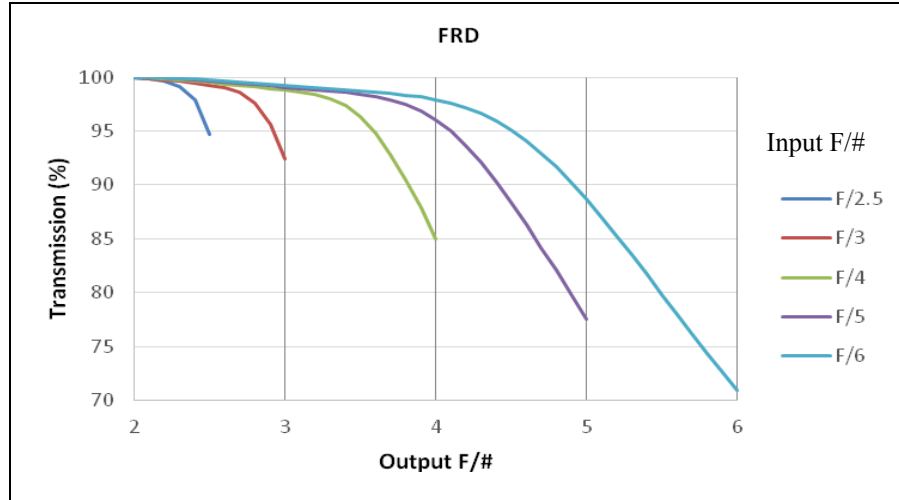


Figure 13 FRD curves of bare fibre

The losses due to the FRD with an aperture of F/3.65 in entrance is estimated at 8% at F/3.5

A sample of the prototypes fibres were then tested to measure the FRD of end-to-end system and the results are shown in Fig. 14.

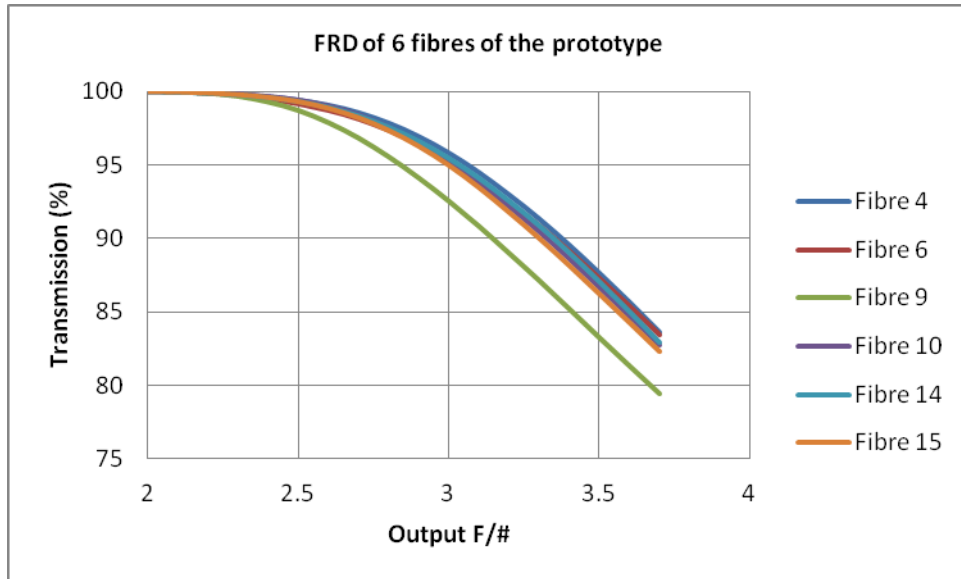


Figure 14 FRD curves of prototype end-to-end fibre system

The average of the losses due to the FRD with an aperture of F/3.65 in entrance is estimated at 14% at F/3.5

#### 4.2 Transmission measurement

The same fibre test bench, as shown in Fig. 12, could also be used to measure the absolute transmission and the results for six test fibres are shown in Fig. 15.

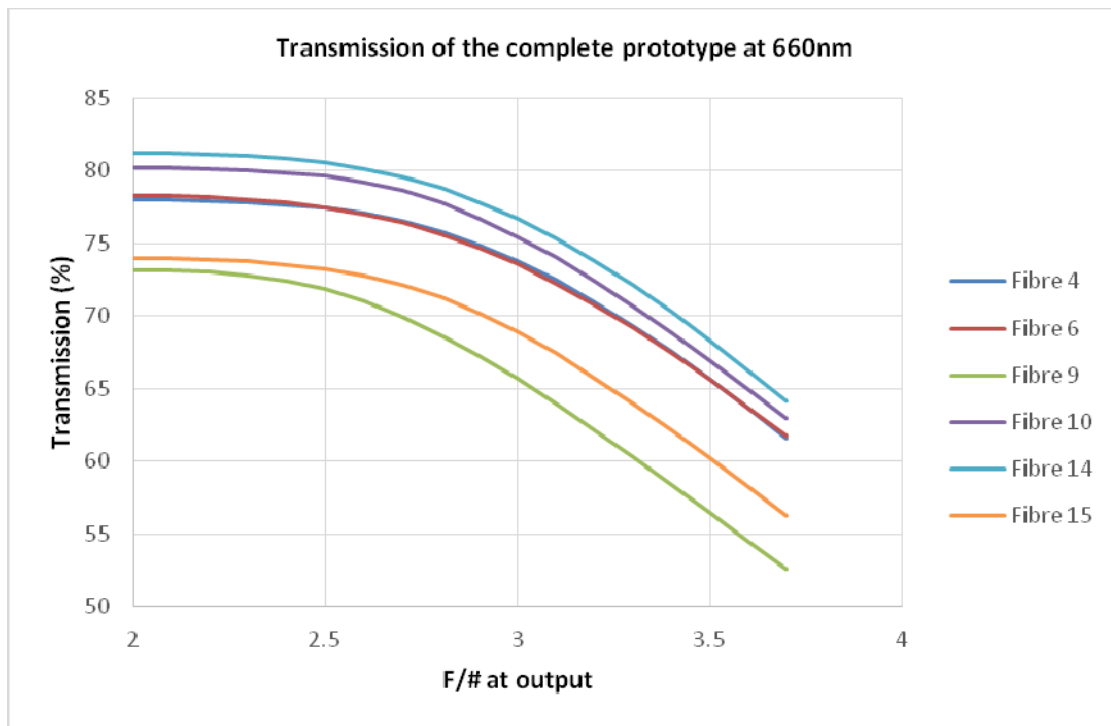


Figure 15 Intrinsic transmission curves of prototype fibres

These results take into account all the effects: gluing of the entrance input, gluing at the connector, vacuum feed-through, gluing at the slitlet and different kinds of tubing.

The important standard deviation is probably due to the difference of the size between the fibre (180 $\mu\text{m}$  on the cladding) and the hole of the connector (195 $\mu\text{m}$ ). The maximum decentring is 15 $\mu\text{m}$  which corresponds to a loss of 13%. For the final design, the size of the fibre should be adapted to the size of the hole in order to minimise these losses.

The global transmission shown in Fig. 15 is improved by 9% for the fibre 14 and 15% for the fibre 9 at F/3.5 with the use of index matching gel (which eliminates Fresnel losses and the imperfection of the polishing of the connector). The results are shown in Fig. 16.

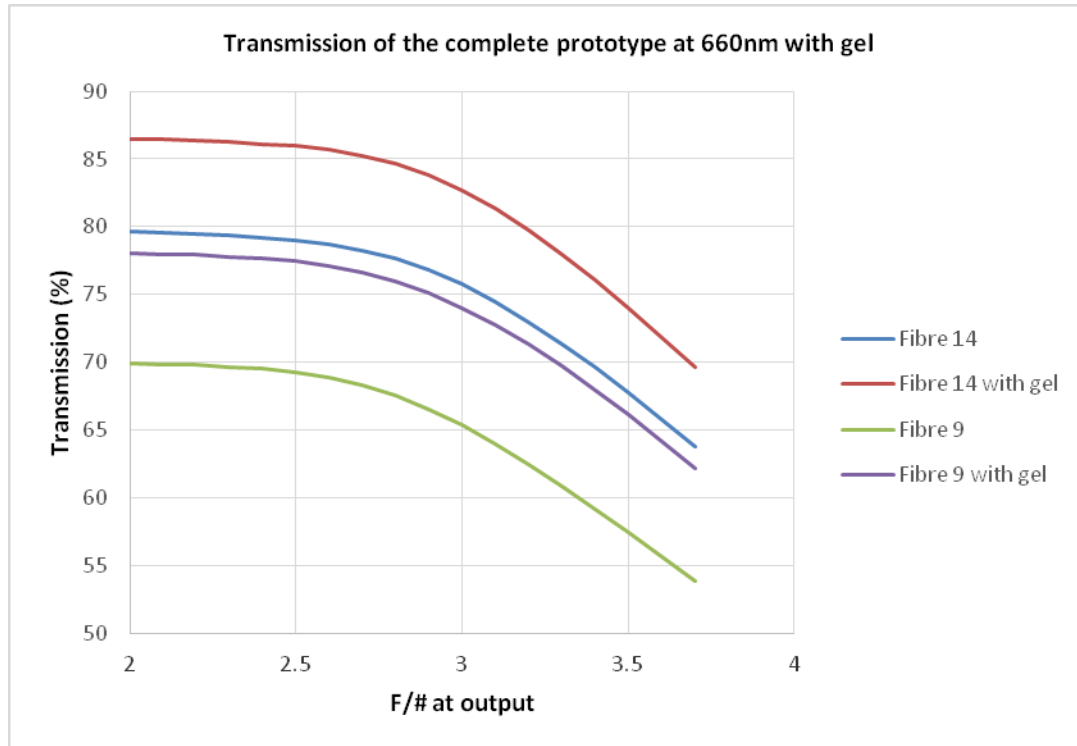


Figure 16 Intrinsic transmission curves of prototype fibres with index matching gel

### 4.3 Fibre Twist FRD measurements

Each MOONS fibre is attached to a robotic Fibre Positioning Unit (FPU) which utilises two motorised rotating arms [ref 2] to position the fibre within a 50 mm diameter pick off field. As the arms rotate the fibre can be subjected to changing mechanical stress as it coils around the hardware. To check the effect of the FPU motion on the FRD of the fibre a 1m test fibre was attached to a prototype FPU to allow the FRD performance as a function of FPU position to be measured. The layout of the FPU and test equipment used in the FRD test is shown in Fig. 17. The test fibre is routed through the FPU arm as it would be in the MOONS instrument. Input illumination is provided by an integrating sphere illuminating an F/3.3 input lens (not shown in Fig.17 ref [3]). The output beam from the fibre, indicated by the orange arrow in Fig. 17, is measured using a test camera operating in the RI-band. The results of FRD tests with the FPU in its datum position (shown in Fig. 17), rotated fully anti-clockwise, and rotated fully clockwise showed a peak to valley variation of less than 2% in throughput, measured within an F/3.3 output beam. The FRD variation is within permissible limits.

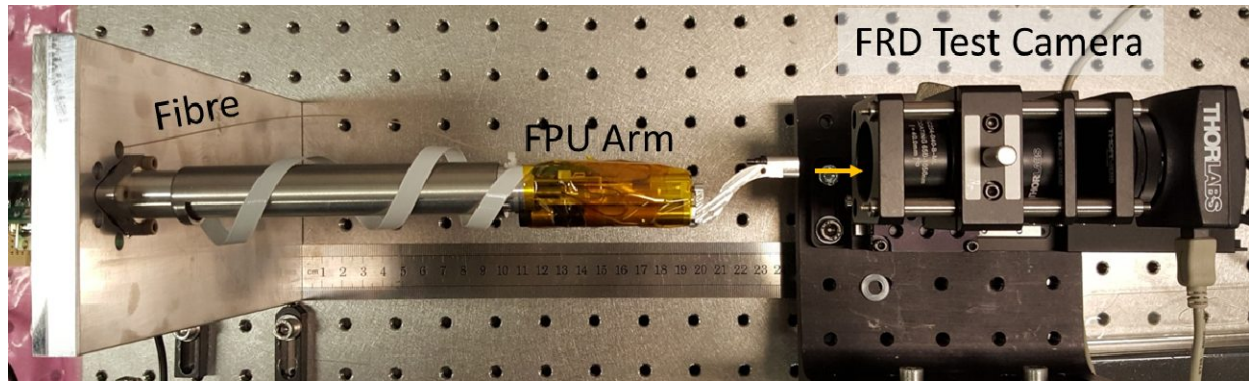


Figure 17 Picture of a test fibre mounted on to a Fibre Positioning Unit (FPU)

A life test was then performed where the FPU was driven through its full range of travel, continuously, until the FPU performance began to fail. At regular intervals during the life test the FPU motion was temporarily paused to enable an FRD test to be performed. The measured FRD variation over the 11 week period of the life test is shown in Fig. 18. The average throughput, measured with an F/3.3 output cone, is 73.7%, with a peak to valley variation of 2.4%. During the test period the FPU completed in excess of 100,000 positioning moves, equivalent to an on telescope lifetime of TBD years, and the fibres showed no significant change in FRD during this time.

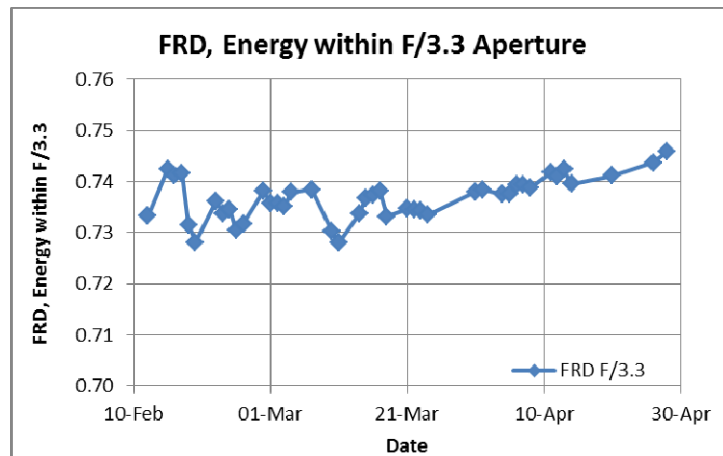


Figure 18 FRD test results for the test fibre attached to the fibre positioning unit.

## 5 CONCLUSION

In this paper, we have described the design of the MOONS fibre developed during Phase B. The table below summarizes the principal technical requirements for the fibre assemblies:

Number of fibres	1024
Number of bundles	64 bundles of 16 fibres
Fibre length	10 m
Sky aperture	1.05 arcsec
Fibre diameter	150/180/210 $\mu\text{m}$
Wavelength range	0.64 – 1.8 $\mu\text{m}$
Input numerical aperture (conversion realized with coupling microlens)	Nasmyth: F/15 to F/3.65 into the fibres
Output numerical aperture	F/3.5
Inter object spacing	5 dark pixels (2.66 x $\emptyset$ fibre core)

*Table 1 Summary matrix*

These tests show that the absolute transmission end-to-end transmission of the fibre without the microlens, including Fresnel losses, internal transmission, FRD and connector with gel is 70% (average) at F/3.65 and collected at F/3.5 at 660nm. Furthermore the FRD has been shown to be unaffected by the motion of the fibre positioning unit and is stable over the expected life time of the MOONS instrument.

The study of the fibre system is based on a close collaboration with the overall project team and also with industry in order to avoid delays, and to reduce costs and eliminate risks during the manufacturing and integration phase.

## REFERENCES

- [1] Cirasuolo M., et al. “MOONS: an optical and near-IR multi-object spectrograph for the very Large telescope”, Proc. SPIE 9147 (2014).
- [2] Montgomery D., et al. “Development of the fibre positioning unit of MOONS”, Proc. SPIE 9908 (2016).
- [3] Guinouard I., et al. “Development of the fibres of MOONS”, Proc. SPIE 9151 (2014).
- [4] Avila G., “FRD and scrambling properties of recent non circular fibres” Proc. SPIE 8446 (2012)